ELSEVIER

Journal of Photochemistry and Photobiology A: Chemistry 140 (2001) 255–262

Journal of Photochemistry and Photobiology A:Chemistry

www.elsevier.nl/locate/jphotochem

# Photosensitization of nanocrystalline $TiO_2$ electrodes with II B group metal-ion-bridged self-assembled films of 3,4,9,10-perylenetetracarboxylic acid

Zhong-Sheng Wang [a,b], Chun-Hui Huang [a,*], Fu-You Li [a], Shi-Fu Weng [a], Shu-Ming Yang [a]

[a] *State Key Laboratory of Rare Earth Materials Chemistry and Applications, Peking University–The University of Hong Kong Joint Laboratory in Rare Earth Materials and Bioinorganic Chemistry, Peking University, Beijing 100871, PR China*

[b] *College of Science, Shandong Agricultural University, Tai'an, Shandong 271018, PR China*

Received 20 October 2000; received in revised form 5 January 2001; accepted 9 February 2001

**Abstract**

Self-assembled films (SA films) of 3,4,9,10-perylenetetracarboxylic acid (PTA) (Film P) and II B group metal-ion-bridged PTA (Film PMP, M = $Zn^{2+}$, $Cd^{2+}$, or $Hg^{2+}$) were fabricated on nanocrystalline $TiO_2$ electrodes and characterized with UV–VIS and IR spectra and XPS. Compared with Film P sensitized solar cell, Grätzel cells based on individual PMP electrodes are more efficient regarding photocurrent generation. Synchrotron radiation photoelectron spectroscopy (SRPES) study reveals that those HOMO energy levels of PMP films are greater than that of Film P. The higher HOMO energy levels will lead to higher excited state energy levels that benefit electron injection, and hence, increase efficiencies for photocurrent generation. In view of the invariable valence of $Zn^{2+}$, $Cd^{2+}$, and $Hg^{2+}$ ions, electron injection should be attributed to ligand, but not to the central metal ions, like the case of Ru(II)–bipyridyl complex. 

*Keywords:* 3,4,9,10-Perylenetetracarboxylic acid; HOMO energy; Ligand

## 1. Introduction

Grätzel type solar cells are heavily investigated currently [1–17] due to the high overall energy conversion efficiencies of up to 10% [18–20]. Especially Ru(II)-polypyridyl complexes are playing an important role in the study of mimicking processes in the photosynthetic reaction center [21–27], from which the basic mechanisms for dye-sensitized solar cell were proposed. For dyes worthy applications in dye-sensitized solar cells, high photo-stability is required; otherwise, they will have no good prospects for application. 3,4,9,10-Perylenetetracarboxylic acid (PTA) is no doubt a promising sensitizer for nanocrystalline $TiO_2$ electrodes due to its strong absorption in the visible, high photo-stability [28,29] and ideal adsorption properties. Derivatives of 3,4,9,10-perylenetetracarboxylic dianhydride have been so far used as functional materials in such fields as organic photoconductors [30], solar energy conversion [31], liquid crystal displays [32,33], and photoelectron molecular devices [34]. Additionally, Ferrere et al. [35] have reported the dye sensitization of nanocrystalline tin oxide by PTA, but few studies on PTA sensitized solar cells based on nanocrystalline $TiO_2$ film have been reported so far.

Moreover, four carboxylic acid groups attached to the opposite sides of perylene renders the possibility of its alternative self-assembly on the surface of $TiO_2$ through metal ions. PTA can adsorb on $TiO_2$ through coordination of $Ti^{4+}$ with two carboxylic acid groups on one side. The other two carboxylic acid groups on the other side can coordinate with suitable metal ions that successively bind a new layer of PTA through coordination bond. Complexes (PMP) can be formed as a result of self-assembly. Therefore, comparison of photoelectric response between PTA sensitized and PMP sensitized solar cells is an interesting topic. Herein, we report the fabrication of alternative self-assembled (SA) films of PTA on porous $TiO_2$ films through II B group metal ion as a bridge. After studying photoelectric conversion properties of nanostructured $TiO_2$ electrode sensitized with PTA itself or SA films of metal-ion-bridged PTA, some interesting results were obtained.

Mononuclear complexes with ligand PTA are difficult to synthesize in conventional solution reactions because carboxylic acid groups on both sides can coordinate with metal ions in opposite directions and usually they form polymer, however, this can be achieved through self-assembly

* Corresponding author. Tel.: +86-10-62757156; fax: +86-10-62751708.
*E-mail address:* hch@chemms.chem.pku.edu.cn (C.-H. Huang).

1010-6030/01/$ – see front matter 
PII: S1010-6030(01)00411-7

technique. The self-assembly method is a good way to obtain artificial novel materials according to one's idea, and their relatively organized structure makes it convenient to carry out characterization and property studies.

## 2. Experimental details

### 2.1. Materials

Propylene carbonate (PC), 3,4,9,10-perylenetetracarboxylic dianhydride and titanium tetraisopropoxide were purchased from Acros. The redox electrolyte used in this work was 0.5 M LiI + 0.05 M $I_2$ in PC. 3,4,9,10-Perylenetetracarboxylic acid (PTA) was prepared by hydrolysis of 3,4,9,10-perylenetetracarboxylic dianhydride [36] and its purity was confirmed by elemental analysis and IR spectrum. Compounds LiI, $I_2$, $ZnCl_2$, $CdCl_2$, and $HgCl_2$ were all of analytical reagent grade (Beijing Chemical Factory, China). Adequate quantity of $ZnCl_2$, $CdCl_2$, or $HgCl_2$ was dissolved in ethanol, respectively, and 1 mM stock solutions were formed. Optically transparent conducting glass (CTO glass, fluorine-doped $SnO_2$ overlayer, transmission greater than 70% in the visible, sheet resistance 20 Ω/sq) was obtained from the Institute of Nonferrous Metals of China.

### 2.2. Preparation of $TiO_2$ Film

Conducting glass substrates were pretreated [12–15] prior to preparation of nanocrystalline $TiO_2$ electrode. The CTO glass substrates were immersed in a saturated solution of KOH in 2-propanol overnight, rinsed with acetone, ethanol and doubly deionized water successively, and dried in an air stream. The total amount of 100–150 g $dm^{-3}$ $TiO_2$ colloid was prepared by following the reported procedure [18]. In order to improve the ohmic contact between $TiO_2$ particles and CTO glass, three drops of $1 \times 10^{-3}$ M titanium tetraisopropoxide in 2-propanol was spread on the conducting glass (2 cm × 8 cm) and dried naturally in air at room temperature. The 7 μm thick nanostructured $TiO_2$ films were fabricated by spreading the adhesive $TiO_2$ colloid onto the first layer and annealed at 450°C for 30 min. For IR measurement, 2 μm thick $TiO_2$ film was deposited on single-crystal silicon (face1 0 0. Transmission is about 20% in the IR region studied). Film thickness was determined with DEKTAK 3 profilometer.

### 2.3. Fabrication of self-assembled films

1. Film P: after $TiO_2$ film was soaked in $3 \times 10^{-4}$ M solution of PTA in DMSO for 3 h, coloration was completed. Thereafter, the electrode was withdrawn from the solution, washed with ethanol for at least six times, and dried in airflow. The $TiO_2$ film that adsorbed monolayer of PTA molecule was denoted as Film P.
2. Film PM: Film P was soaked in 1 mM solution of $ZnCl_2$, $CdCl_2$, or $HgCl_2$ in ethanol, respectively, and Film PM was formed after 3 h. After completion of fabrication, washing and drying procedures are the same as above.
3. After Film PM was soaked in $3 \times 10^{-4}$ M solution of PTA in DMSO for 3 h, Film PMP was fabricated. Immediately following the fabrication are the washing and drying procedures as described above.

Note that 3,4,9,10-perylenetetracarboxylic dianhydride cannot be adsorbed to the surface of nanocrystalline $TiO_2$ under the experimental condition. Therefore, PTA, but not the dianhydride, was chosen as sensitizer.

### 2.4. Photoelectrochemical measurement

The photoelectrochemical experiments were performed in a standard 2-electrode-system described elsewhere [19,37] with 7 μm thick $TiO_2$ electrodes unless specified. The dye-coated film was used as working electrode with effective area of 0.14 $cm^2$. The counter electrode was ITO glass on which 200 nm thick layer of Pt was deposited by sputtering. A thin layer sandwich-type solar cell was fabricated by clamping both electrodes tightly followed by introducing one drop of the redox electrolyte into the interelectrode space. A 500 W xenon lamp (Ushio Electric, Japan) served as a light source in conjunction with an IRA-25S filter to cut off infrared light. A set of band-pass filters (Schott, USA) was set into the path of the excitation beam to adjust the excitation wavelength. Light intensities were measured with a Light Gauge Radiometer/Photometer (Coherent, USA) when an IRA-25S filter, a GG420 cut-off filter (for white light output only) or a band-pass filter (for monochromatic light output only), and a sheet of CTO glass were set in the light beam. Here, an IRA-25S filter was used to filter off infrared light to protect the electrode from heating, and a GG420 cut-off filter was used to cut off the light with wavelength less than 420 nm to avoid the excitation of $TiO_2$ by ultraviolet light. Note that light intensities measured in this work have been corrected for scattering and absorption by CTO glass as a result of a sheet of CTO glass set in the light beam when light intensities were measured.

### 2.5. Instrumentation

The UV–VIS spectra were measured with a Shimadzu model 3100 UV–VIS–NIR spectrophotometer, and IR spectra were recorded on a Nicolet MAGNA-IR 750 Spectrometer. In order to minimize the systematic error, a series of SA films (i.e. from P to PMP) were fabricated successively on the fixed nanocrystalline $TiO_2$ film, and each fabrication of SA film was followed by UV–VIS or IR measurement immediately. XPS was performed on VGESCA LAB 5 Multitechnique photoelectron spectrometer (VG. CO., UK) using Al Kα as radiation. Synchrotron radiation photoelectron spectroscopy (SRPES) was measured on

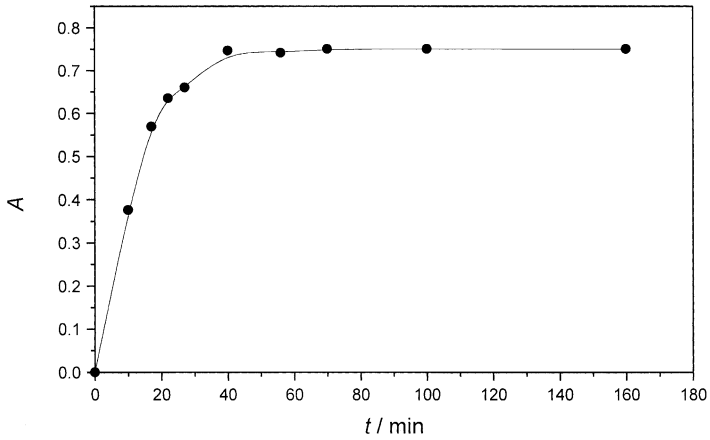


Fig. 1. Relationship of maximum absorbance of Film P with sensitization duration. $TiO_2$ film used here was about 2 μm thick. Absorbance has been corrected for the absorption of $TiO_2$ film and glass support.

photon–electron spectrometer (vsw Scientific Instruments Ltd., Eng.) through synchrotron radiation. Under ultravacuum (3–4 × $10^{-8}$ Pa), photoelectron spectra were recorded under 62 eV synchrotron radiation light, from which the first ionization energy, the HOMO energy level, was derived for different SA films.

## 3. Results and discussion

### 3.1. Film P

#### 3.1.1. Adsorption behavior

A nanocrystalline $TiO_2$ film was soaked into a PTA solution in DMSO, and withdrawn from the solution for absorbance determination at variable time intervals. The sensitized film was washed thoroughly with anhydrous ethanol and dried in airflow followed by the measurement. Fig. 1 shows the relationship of maximum absorbance and the sensitization-duration. Adsorption can be divided into three stages. Since pores in the $TiO_2$ film are all unoccupied at the initial stage of adsorption, adsorbance is increased rapidly, Then the adsorption rate is slowed down with the increase of adsorbance. Finally, adsorption reaches saturation when all active surface is occupied. One can see from Fig. 1 that the optimal duration for sensitization is greater than 40 min. In order to ensure adsorption saturation, 3 h-sensitization was chosen in this work.

#### 3.1.2. UV–VIS spectra

The absorption spectra of PTA in DMSO and Film P are shown in Fig. 2. The PTA exhibits four characteristic peaks in the visible. The strong absorption in the visible is resulted from the large planar structure with π-conjugation system. Upon adsorption of PTA on porous $TiO_2$ film, only two peaks appear in the spectrum due to the overlap of absorption peaks. Comparison of the spectrum of Film P with that of PTA in DMSO reveals that absorption is well extended to the

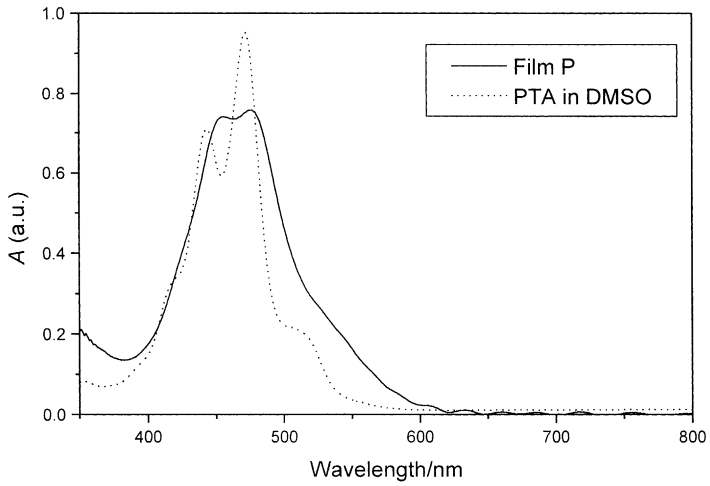


Fig. 2. The UV–VIS spectra for PTA in DMSO (dotted line) and Film P (solid line). $TiO_2$ film used here was about 2 μm thick. Absorption for $TiO_2$ film and glass support has been deducted for Film P.

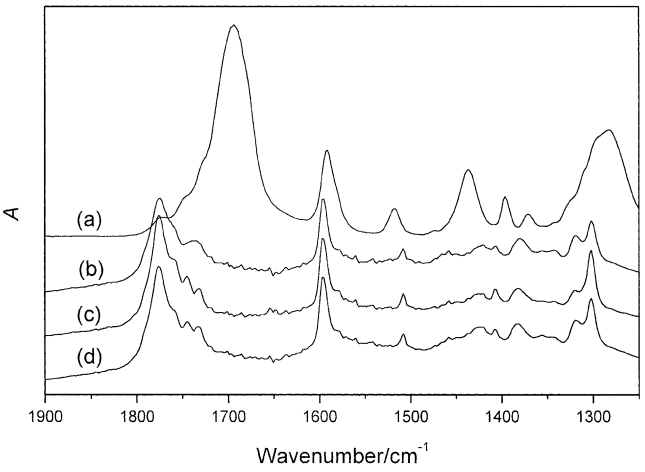


Fig. 3. The IR spectra for (a) PTA (solid); (b) Film P; (c) Film PZn; and (d) Film PZnP. IR spectrum of PTA (solid) was measured by means of microscope IR and spectra of SA films were measured directly on $TiO_2$ films deposited on single-crystal silicon (face 1 0 0). Absorption intensity of spectra is normalized to the peak intensity of C=C stretch in order to compare the relative intensity of the bands in the wavenumber region between 1900 and 1250 $cm^{-1}$.

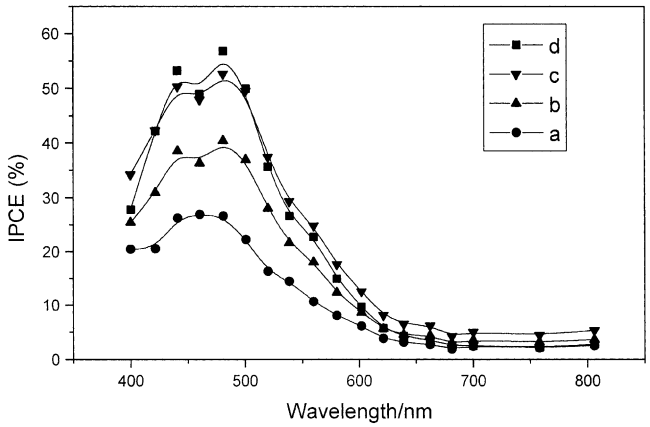


Fig. 4. Photocurrent action spectra for (a) Film P; (b) Film PHgP; (c) Film PCdP; and (d) Film PZnP.

red region. The red shift of absorption threshold indicates the charge-transfer transition involved between PTA and $Ti^{4+}$ ion, and the effect is interpreted in terms of an increase in the delocalization of the π orbital of the PTA ligand upon adsorption of PTA to the surface of $TiO_2$ [19].

### *3.1.3. IR spectra*

The carboxylic acid is known to interact with $TiO_2$ surfaces through chemical bond formation to the surface, chelating or bridging modes, or physical adsorption [38]. Interfacial binding between the dye molecules and $TiO_2$ surface was characterized by IR spectra of the SA-film-coated $TiO_2$ films. Fig. 3(a) shows the microscope IR spectrum of PTA powder. Absorption peaks at 1591, 1284 and 1693 $cm^{-1}$ (Table 1) were attributed to C=C stretch mode of perylene and C–O and C=O stretch modes of the carboxylic acid group in dimer, respectively. The spectrum of Film P (Fig. 3(b) has two peaks at 1776 and 1734 $cm^{-1}$, respectively, which are the characteristic absorption peaks of carboxylic acid group in monomer: the former for free groups and the latter for coordinated ones. Consequently, it is inferred that monolayer of PTA is adsorbed onto $TiO_2$. Similarly, there are two peaks for C–O stretch modes at 1319 and 1302 $cm^{-1}$, respectively. 1319 $cm^{-1}$ is assigned to free carboxylic acid groups and 1302 $cm^{-1}$ for coordinated ones in the case of interaction mode as O=C–O–Ti [38]. Two carboxylic acid groups on one side of PTA can interact with $TiO_2$ surfaces and the other two groups are free in the ideal case. However, it is not the case. The peak at 1776 $cm^{-1}$ is stronger than that at 1734 $cm^{-1}$. Therefore, it is implied that more free carboxylic acid groups than coordinated ones exist in Film P. This result can be rationalized by the fact that in some cases only one of the four carboxylic acid groups is involved in coordination due to the steric hindrance.

### *3.1.4. PTA sensitized photocurrent generation*

Fig. 4(a) shows the action spectrum of PTA sensitized solar cell, where IPCE is plotted as a function of incident

Table 1
The IR absorption properties and major XPS peaks of metal-ion-bridged SA films

| | PTA | P | PZnP | PCdP | PHgP |
|---|---|---|---|---|---|
| Binding energy (eV) | | | 1044.8 ($Zn2p_{1/2}$), 1021.7 ($Zn2p_{3/2}$) | 411.6 ($Cd3d_{3/2}$), 404.8 ($Cd3d_{5/2}$) | 102.0 ($Hg4f_{5/2}$), 96.9 ($Hg4f_{7/2}$) |
| IR[a] | | | | | |
| ν (C=C) ($cm^{-1}$) | 1591 | 1597 | 1597 | 1597 | 1597 |
| ν (C=O) ($cm^{-1}$) | 1693 | 1776 | 1776 | 1776 | 1776 |
| | | – | 1759 | 1759 | 1759 |
| | | – | 1744 | 1744 | 1744 |
| | | 1734 | 1732 | 1732 | 1730 |
| ν (CO) + δ (COOH) ($cm^{-1}$) | 1284 | 1319 | 1319 | 1319 | 1319 |
| | | 1302 | 1302 | 1302 | 1302 |

[a] The IR spectrum of PTA was measured by means of microscope IR. The IR spectra for SA films were measured directly on $TiO_2$ film deposited on single-crystal silicon.

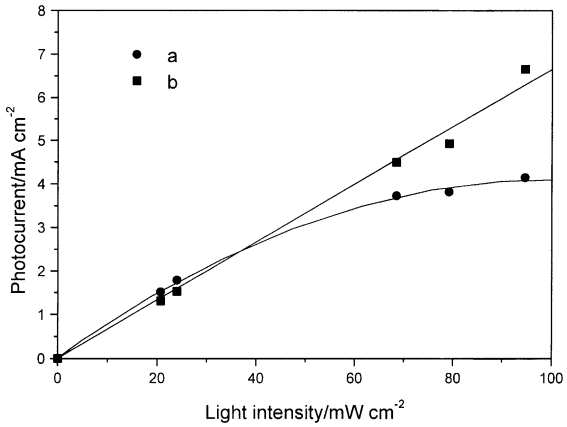


Fig. 5. Relationship between short-circuit photocurrents and light intensities for (a) Film P and (b) Film PZnP. Sandwich-type solar cells were under illumination of white light from a Xe lamp whose infrared and ultraviolet light was cut off with an IRA-25S and a GG420 cut-off filters.

wavelength [19]. The PTA anchored to the $TiO_2$ surface is responsible for the photocurrent generation owing to the resemblance of action spectrum to UV–VIS spectrum. Under monochromatic incident light, sandwich-type solar cell generated steady anodic photocurrents, and the maximum IPCE (26.9%) appeared at 480 nm. One can infer from the low IPCE data that charge recombination, resulted from the mismatch between excited state energy level of PTA and the conduction band energy level of $TiO_2$ and or the large rate constant for the back reaction with respect to electron injection, is serious in this system. It is expected that IPCE will be increased significantly after reducing charge recombination.

The effect of light intensity on the short-circuit photocurrents was examined, as seen in Fig. 5(a). The short-circuit photocurrents increase nonlinearly with light intensities. Especially photocurrents increase less than expected with increasing light intensity from 24 mW $cm^{-2}$. The relationship of photocurrents with light intensities indicates that diffusion is not fast enough to reduce dye cations; this is also a reflection of serious charge recombination present in this system.

## 4. Film PM and Film PMP

### 4.1. XPS spectra

The XPS is a powerful means to detect metal ions in films. Characteristic XPS peaks observed for the three metal ions confirms the existence of metal ions in the corresponding PMP films, and they are listed in Table 1. For Film PZnP, peaks at 1044.8 and 1021.7 eV are assigned to $Zn2p_{1/2}$ and $Zn2p_{3/2}$, respectively. The distance of 23.1 eV between the two peaks further confirms the existence of $Zn^{2+}$ in Film PZnP. Similarly, the characteristic XPS peaks for $Cd^{2+}$ and $Hg^{2+}$ were also observed for Film PCdP and PHgP, respectively, as seen in Table 1.

### 4.2. IR-spectra

Three PM films show similar features of IR spectrum so do the three PMP films. The data for major IR peaks of PMP films are listed in Table 1. In order to discuss spectrum changes conveniently, IR spectra for Film PZn and PZnP, as representatives, are also shown in Fig. 3. Compared with Film P, there are more kinds of carboxylic acid groups in Film PZn. The carboxylic acid groups can coordinate with $Ti^{4+}$ or $Zn^{2+}$ ion and can be free. The two more peaks appearing at 1759 and 1744 $cm^{-1}$ (Fig. 3(c)) should be related to the C=O stretch modes resulted from the coordination of PTA and $Zn^{2+}$ ion. Different coordination bond lengths and different interaction modes between carboxylic acid groups and $TiO_2$ surface or $Zn^{2+}$ ions will result in more than one peak for the C=O stretch modes. That the 1776 $cm^{-1}$ also appears in Film PZn further supports some carboxylic acid groups uninvolved in coordination due to the steric hindrance; this is understandable in the case of nanopores. For Film PZnP, another layer of PTA is adsorbed through two carboxylic acid groups on one side coordinating with $Zn^{2+}$, and the other two groups on the other side are free. Consequently, four peaks at 1776, 1759, 1744 and 1732 $cm^{-1}$ appear in the spectrum of PZnP film (Fig. 3 (d)). Interestingly, the relative intensity of the 1302 $cm^{-1}$ peak increases from Film P to Film PZn as a result of relatively increased number of coordinated carboxylic acid groups, and then decreases from Film PZn to Film PZnP as a result of relatively decreased number of coordinated carboxylic acid groups.

### 4.3. UV–VIS spectra

Electronic spectra for Film PZn and PZnP are present in Fig. 6. The pronounced increase in absorbance from Film PZn to Film PZnP indicates that $TiO_2$ adsorbs another layer of PTA, both layers of PTA connected through coordination bonds between carboxylic acid groups and $Zn^{2+}$ ions.

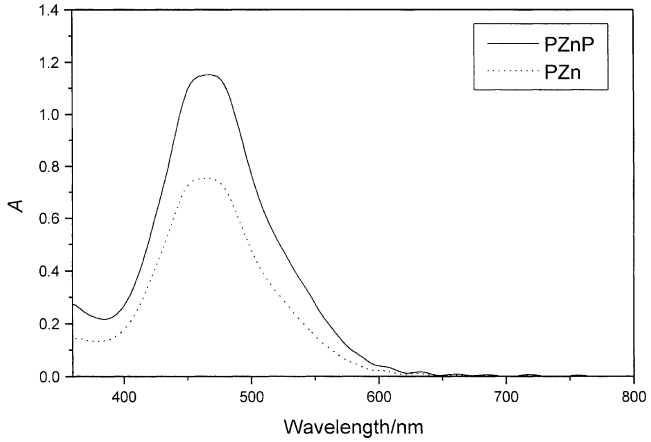


Fig. 6. The UV–VIS spectra for Film PZn (dotted line) and Film PZnP (solid line). Absorbance has been corrected for the absorption of $TiO_2$ film and glass support. $TiO_2$ film used here was about 2 μm thick.

Table 2
Adsorbed amount of PTA, IPCE data and energy levels for different SA films

| | P | PZnP | PCdP | PHgP |
|---|---|---|---|---|
| Molecules/film ($cm^2$)[a] | $4.27 \times 10^{16}$ | $6.22 \times 10^{16}$ (45.7%)[b] | $6.49 \times 10^{16}$ (52.0%) | $6.28 \times 10^{16}$ (47.1%) |
| $IPCE_{max}$ (%) | 26.9 | 56.8 | 52.6 | 40.4 |
| HOMO energy level (eV) | −6.79 | −6.53 | −6.57 | −6.64 |
| Excited energy level (eV) | −4.20 | −3.94 | −3.98 | −4.05 |

[a] $TiO_2$ films used here were 7 μm thick, extinction coefficient of PTA in 0.1 M NaOH aqueous solution was measured to be $4.46 \times 10^4\ M^{-1}\ cm^{-1}$.
[b] Values in parentheses stand for the increase in adsorbed amount of PTA from Film P to Film PMP.

Film P only contains monolayer of PTA confirmed by the IR spectrum of Film P (see IR analyses). Metal ions are adsorbed by coordinating with carboxylic acid groups and subsequently connect another layer of PTA through coordination bond too when Film PM is dipped in PTA solution. As absorbance of PTA on the surface of $TiO_2$ cannot be increased by prolonging sensitization duration (see Fig. 1), the notable increase of absorbance for Film PZnP with respect to Film PZn confirms another layer of PTA adsorbed to the first layer through coordination interaction. MLCT band is not observed from the UV–VIS spectra for both Film PM and Film PZnP. However, this cannot exclude the possibility of complex formation because MLCT band can be covered up by the strong absorption of PTA in the visible.

In order to compare the adsorbance of PTA on $TiO_2$ surface from Film P to Film PMP, PTA was desorbed to 0.1 M NaOH aqueous solution. The amount of PTA was calculated by measuring the absorbance of the above solutions (shown in Table 2). One can see from Table 2 that amount of PTA can be increased from Film P to Film PMP by about 50%. This remarkable increase in amount of PTA from Film P to Film PMP further confirms that another layer of PTA is adsorbed as a result of existence of metal ions.

### 4.4. Photocurrent action spectrum

In order to investigate the effect of metal ion on electron transfer, action spectra for different PMP electrodes were also measured with sandwich-type solar cells. IPCEs are increased to different extent upon formation of PMP films depending on the metal ions, as seen in Fig. 4. One can see from Table 2 that the maximum IPCE at 480 nm is in the following order: PZnP > PCdP > PHgP > P. For PZnP and PCdP electrodes, the maximum IPCE of PZnP or PCdP is approximately doubled with respect to that of electrode P. Obviously, the increased absorbance (∼50%) cannot be responsible for the increased IPCE completely, but the latter can be interpreted by the difference of HOMO energy levels for different SA films. In fact, PMP film can be considered as a kind of complex, which of course differs from the ligand. Metal ions play a different role in complexes that, hence, have different HOMO energy levels. Therefore, the different PMP films show discrepancy in photocurrent generation. The HOMO energy levels relative to vacuum measured with SRPES for different SA films are listed in Table 2, from which one can see that the HOMO energy levels relative to vacuum are −6.53, −6.57, −6.64 and −6.79 eV for PZnP, PCdP, PHgP and P, respectively. Excited state energy levels can be estimated through HOMO energy levels and the maximum absorption wavelength at 480 nm (2.59 eV, corresponding to excitation energy), −4.20 eV for Film P, −3.94 eV for Film PZnP, −3.98 eV for Film PCdP, and −4.05 eV for Film PHgP. The excited state energy levels for all SA films are higher than the bottom of the conduction band (−4.40 eV) of $TiO_2$, indicating electron injection from dyes to the conduction band of $TiO_2$ is thermodynamically possible. The higher excited state energy levels for PMP films, compared with Film P (−4.20 eV), can increase the driving force for electron injection and IPCE is, therefore, increased. For the four electrodes, the higher the excited state energy levels the larger the IPCE.

### 4.5. Photovoltage–current characteristics

Under irradiation of white light (94.6 $mW\,cm^{-2}$) from a Xe lamp, photocurrents and their corresponding photovoltage were measured by adjusting variable resistance. The performance parameters for solar cells based on individual electrodes are listed in Table 3. The fill factor is defined as expression (1):

$$FF = \frac{V_{opt} I_{opt}}{V_{oc} I_{sc}} \tag{1}$$

where $V_{opt}$ and $I_{opt}$ are, respectively, voltage and current for maximum power output. Also $\eta$ is defined as the following equation:

$$\eta = \frac{I_{sc} V_{oc} FF}{P_{in}} \tag{2}$$

Table 3
Performance parameters for sandwich-type solar cells[a]

| | P | PZnP | PCdP | PHgP |
|---|---|---|---|---|
| $I_{sc}$ ($mA\,cm^{-2}$) | 4.14 | 6.65 | 6.04 | 5.42 |
| $V_{oc}$ (mV) | 250 | 308 | 299 | 289 |
| FF | 0.410 | 0.385 | 0.375 | 0.397 |
| $\eta$ (%) | 0.445 | 0.83 | 0.72 | 0.66 |

[a] Conditions: 94.6 $mW\,cm^{-2}$ white light from a Xe lamp; Infrared light and ultraviolet light were cut off with an IRA-25S filter and a GG420 cut-off filter.

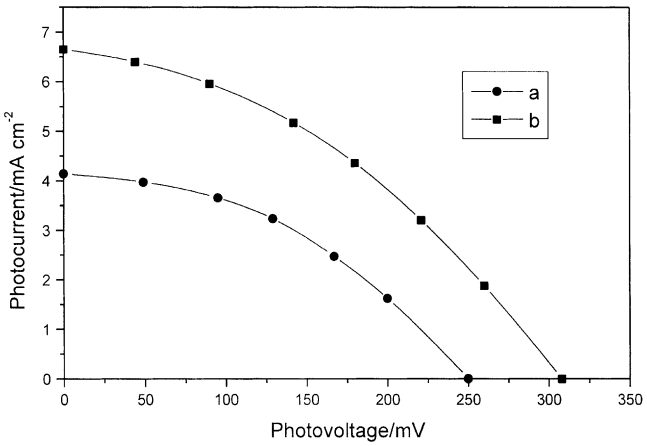


Fig. 7. The *I–V* curves for (a) electrode P and (b) electrode PZnP. Conditions as in Table 3.

where $P_{in}$ is the power of incident white light. $I_{sc}$, $V_{oc}$ and $\eta$ are all in the following order: PZnP > PCdP > PHgP > P, which accords with the IPCE order. Among the four SA films, Film PZnP has the highest short-circuit photocurrent (6.65 mA cm$^{-2}$), open-circuit photovoltage (308 mV) and overall yield (0.83%). The *I–V* curves for Film P and Film PZnP, as an example, are shown in Fig. 7.

The effect of light intensity on short-circuit photocurrent was also examined, as seen in Fig. 5 (b). Unlike Film P, short-circuit photocurrents increased linearly with light intensities for Film PZnP, indicating that photocurrent generation is not limited by diffusion of the iodide or triiodide ions within the nanocrystalline film in the light intensity range studied. One can see from the above analyses that when suitable metal ion was introduced into the interspace of two-layer PTA through coordination bond, photocurrent generation can be improved significantly due to the increase of HOMO energy level.

Four samples for each type of SA film were measured under the same conditions in all photoelectrochemical experiments of this work, and results remained almost unchanged within the range of experimental deviation. Therefore, photoelectrochemical measurements were reproduced well.

## 5. Conclusion

Complexes of II B group metal ions were successfully formed through alternative self-assembly of PTA and metal ions on nanocrystalline $TiO_2$ film. Compared with film P, IPCE is increased significantly upon the formation of Film PMP. The increased IPCE can be interpreted by the increase of HOMO energy level when the complex is formed. For this system, higher HOMO energy levels correspond to higher excited state energy levels, therefore, the driving force for electron injection is increased. It is noted for PMP electrodes that electron should be injected from PTA, but not the central metal ion, to the conduction band of $TiO_2$ because the metal ions used in this work are all of invariable valence. The result provides a new way to improve photoelectric properties for dyes like PTA and is worthy further study.

## Acknowledgements

The State Key Program of Fundamental Research (G 1998061308), the NNSFC (20023005 and 59872001), and Doctoral Program Foundation of Higher Education (99000132) are gratefully acknowledged for the financial support.

## References

[1] A. Solbrand, H. Lindström, H. Rensmo, A. Hagfeldt, S.-E. Lindquist, S. Södergren, J. Phys. Chem. B 101 (1997) 3514.
[2] A. Solbrand, A. Henninggsson, S. Södergren, H. Lindström, A. Hagfeldt, S.-E. Lindquist, J. Phys. Chem. 103 (1999) 1078.
[3] C.J. Barbé, F. Arendse, P. Comte, M. Jirousek, F. Lenzmann, V. Shklover, M. Grätzel, J. Am. Ceram. Soc. 80 (1997) 3157.
[4] G. Will, G. Boschloo, R. Hoyle, S.N. Rao, D. Fitzmaurice, J. Phys. Chem. B 102 (1998) 10272.
[5] A. Kay, R. Humphry-Baker, M. Grätzel, J. Phys. Chem. 98 (1994) 952.
[6] T.A. Heimer, S.T. D'Arcangelis, F. Farzad, J.M. Stipkala, G. Meyer, Inorg. Chem. 35 (1996) 5319.
[7] N.W. Duffy, K.D. Dobson, K.C. Gordon, B.H. Robinson, A.J. McQuillan, Chem. Phys. Lett. 266 (1997) 451.
[8] A.C. Khazraji, S. Hotchandani, S. Das, P.V. Kamat, J. Phys. Chem. B 103 (1999) 4693.
[9] S. Das, P.V. Kamat, J. Phys. Chem. B 103 (1999) 209.
[10] S. Das, P.V. Kamat, J. Phys. Chem. B 102 (1998) 8954.
[11] C. Nasr, S. Hotchandani, P.V. Kamat, J. Phys. Chem. B 102 (1998) 4944.
[12] Z.-S. Wang, F.-Y. Li, C.-H. Huang, L. Wang, M. Wei, L.-P. Jin, N.-Q. Li, J. Phys. Chem. B 104 (2000) 9676.
[13] Z.-S. Wang, C.-H. Huang, B.-W. Zhang, Y.-J. Hou, P.-H. Xie, H.-J. Qian, K. Ibrahim, New J. Chem. 24 (2000) 567.
[14] Z.-S. Wang, Y.-Y. Huang, C.-H. Huang, J. Zheng, H.-M. Cheng, S.-J. Tian, Synth. Met. 114 (2000) 201.
[15] Z.-S. Wang, F.-Y. Li, C.-H. Huang, Chem. Commun. (2000) 2063.
[16] K. Tennakone, G.R.R.A. Kumara, I.R.M. Kottegoda, V.P.S. Perera, Chem. Commun. (1999) 15.
[17] R. Argazzi, C. Bignozzi, T.A. Heimer, F.N. Castellano, G.J. Meyer, J. Phys. Chem. B 101 (1997) 2591.
[18] B. O'Regen, M. Grätzel, Nature (London) 353 (1991) 737.
[19] M.K. Nazeeruddin, A. Kay, I. Rodicio, R. Humphry-Baker, E. Müller, N. Vlachopoulos, M. Grätzel, J. Am. Chem. Soc. 115 (1993) 6382.
[20] P. Péchy, F.P. Rotzinger, M.K. Nazeeruddin, O.S. Kohle, M. Zakeeruddin, R. Humphry-Baker, M.J. Grätzel, Chem. Soc., Chem. Commun. (1995) 65.
[21] E. Zahavy, M. Seiler, S. Marx-Tibbon, E. Joselevich, I. Willner, H. Dürr, D. O'Connor, A. Harrimann, Angew. Chem. 107 (1995) 112.
[22] A. Magnusson, B. Akermark, S. Styring, L. Sun, J. Am. Chem. Soc. 119 (1997) 10720.
[23] S. Bossmann, R. Schwarz, M. Kropf, R. Hayo, J. Photochem. Photobiol. A: Chem. 80 (1994) 341.
[24] M. Seiler, H. Dürr, Liebigs Ann. (1995) 407.
[25] M. Kropf, D. van Loyen, O. Schwarz, H. Dürr, J. Phys. Chem. A 102 (1998) 5499.
[26] Y.Z. Hu, S.H. Bossmann, D. van Loyen, O. Schwarz, H. Dürr, Chem. Eur. J. 5 (1999) 1137.
[27] A.C. Benniston, P.R. Mackie, A. Harriman, Angew. Chem. 110 (1998) 376.

[28] I. Lukac, H. Langhals, Chem. Ber. 116 (1983) 3524.
[29] W.E. Ford, P.V. Kamat, J. Phys. Chem. 91 (1987) 6373.
[30] K.C. Nguyen, D.S. Weiss, J. Imag. Technol. 15 (1989) 158.
[31] S.R. Forrst, et al., J. Appl. Phys. 55 (1984) 1492.
[32] S. Roland, Dyes Pigment 24 (1994) 295.
[33] R.L. Vanewyk, et. al., Display 10 (1986) 155.
[34] M.P. O'Neil, M.P. Niemczyk, W.A. Svec, D. Gosztola, G.L. Gaines III, M.R. Wasielewski, Science 257 (1992) 63–65.
[35] S. Ferrere, A. Zaban, B.A. Gregg, J. Phys. Chem. B 101 (1997) 4490.
[36] E. Keh, B. Valeur, J. Colloid Interface Sci. 79 (1981) 465.
[37] G.P. Smestad, M. Grätzel, J. Chem. Educ. 75 (1998) 752.
[38] T.J. Meyer, G.J. Meyer, B.W. Pfennig, J.R. Schoonover, C.J. Timpson, J.F. Wall, C. Kobusch, X.H. Chen, B.M. Peek, C.G. Wall, W. Ou, B.W. Erickson, C.A. Bignozzi, Inorg. Chem. 33 (1994) 3952.